JOC The Journal of Organic Chemistry
Cite This: J. Org. Chem. 2019, 84, 3552−3558
Article
pubs.acs.org/joc

# (2,5-Dioxoimidazolidin-4-ylidene)aminocarbonylcarbamic Acid as a Precursor of Parabanic Acid, the Singlet Oxygen-Specific Oxidation Product of Uric Acid

Sayaka Iida, Yorihiro Yamamoto, and Akio Fujisawa*

School of Bioscience and Biotechnology, Tokyo University of Technology, 1404-1 Katakura-cho, Hachioji, Tokyo 192-0982, Japan

**ABSTRACT:** Previously, we identified that parabanic acid (PA) and its hydrolysate, oxaluric acid (OUA), are the singlet oxygen-specific oxidation products of uric acid (UA). In this study, we investigated the PA formation mechanism by using HPLC and a time-of-flight mass spectrometry technique and identified unknown intermediates as (2,5-dioxoimidazolidin-4-ylidene)-aminocarbonylcarbamic acid (DIAA), dehydroallantoin, and 4-hydroxyallantoin (4-HAL). DIAA is the key to PA production, and its formation pathway was characterized using $^{18}O_2$ and $H_2{}^{18}O$. Two oxygen atoms were confirmed to be incorporated into DIAA: the 5-oxo- oxygen from singlet oxygen and the carboxylic oxygen from water. Isolated DIAA and 4-HAL gave PA stoichiometrically. A plausible reaction scheme in which two pathways branch out from DIAA is presented, and the potential for PA as an endogenous probe for biological formation of singlet oxygen is discussed.

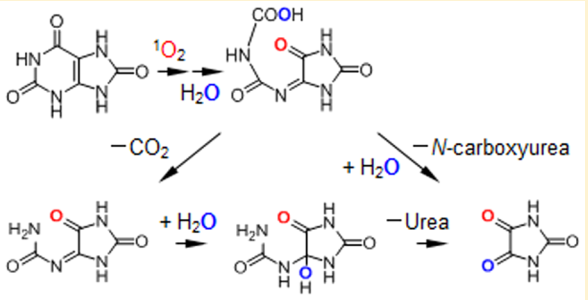




## INTRODUCTION

The ability to detect reactive oxygen species (ROS) or reactive nitrogen species (RNS) in pathological events is highly desired, since they are considered to play a key role in many diseases. Monitoring end products of these reactive species and substrates, such as lipids, proteins, and nucleic acids, is a reasonable way for identifying ROS and RNS in vivo because these species are too unstable to detect directly. We believe that uric acid (UA) is an ideal endogenous probe for this purpose because it exists ubiquitously in human bodily fluids at relatively high concentrations (e.g., ∼300 $\mu M$ in plasma[1]) and reacts with ROS and RNS, yielding different products (see additional details later in this section).

UA is an interesting molecule. It is a terminal metabolite of purine in primates including humans and also an essential water-soluble antioxidant. UA gives specific oxidation products after its reaction with various ROS and RNS. Allantoin (AL)[1,2] is produced by free radical-induced oxidation, triuret (TU)[3,4] by $ONOO^-$, 6-aminouracil (6-AU)[5] by $^{\bullet}NO$, 5-*N*-carboxyimino-6-*N*-chloroaminopyrimidine-2,4(3*H*)-dione (CCPD)[6] by hypochlorous anion ($ClO^-$), and parabanic acid (PA)[7] by singlet oxygen ($^1O_2$) (Figure 1). Obviously, the products are different depending on the ROS and RNS; therefore, UA can function as an endogenous probe for each ROS and RNS.

In our previous study,[7] we identified PA and its hydrolysate, oxaluric acid (OUA), as the $^1O_2$-specific oxidation products of UA and confirmed no other ROS or RNS gave PA and OUA as products. However, the PA formation pathway remains unclear. We also found an intermediate (U3, $m/z$ −199.01072) but could not fully characterize it. In this study, we succeeded in identifying U3 as (2,5-dioxoimidazolidin-4-ylidene)aminocarbonylcarbamic acid (DIAA) and two other intermediates (U4 and U5) as dehydroallantoin

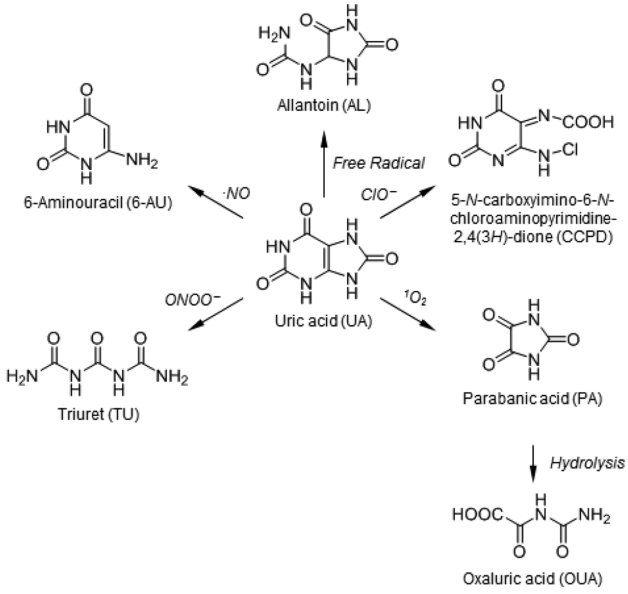


**Figure 1.** Oxidation products of UA induced by various ROS and RNS. AL is produced by free-radical-induced oxidation; 6-AU by $^{\bullet}NO$; TU by $ONOO^-$; CCPD by $ClO^-$; and PA and its hydrolysate OUA by $^1O_2$.

**Received:** January 16, 2019
**Published:** February 26, 2019





DOI: 10.1021/acs.joc.9b00163
J. Org. Chem. 2019, 84, 3552−3558

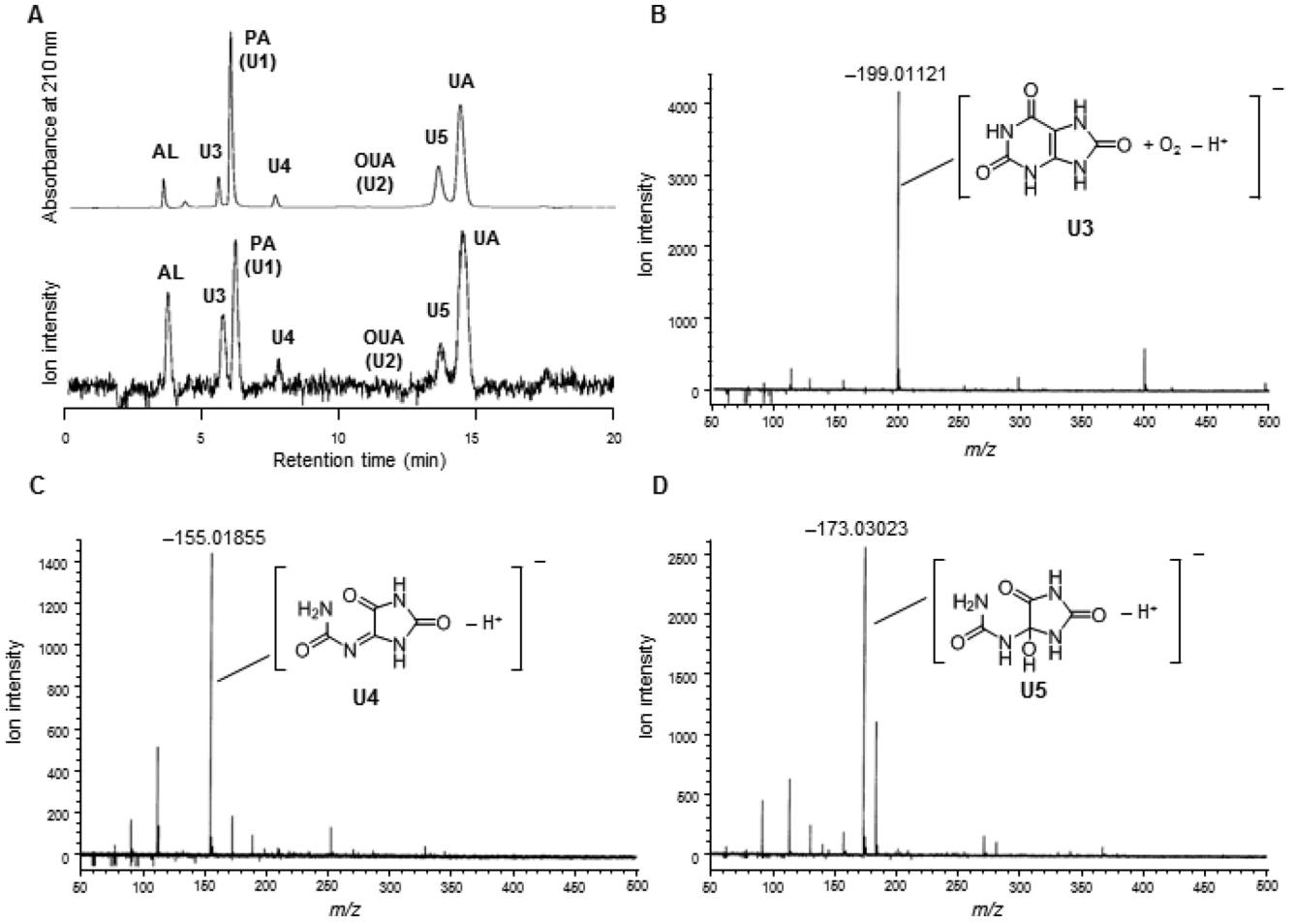


**Figure 2.** HPLC chromatograms of reaction mixture after 60 min of UA photooxidation induced by 10 $\mu$M rose bengal and UVA irradiation (1.12 mW/cm$^2$) and MS spectra of observed products U3, U4, and U5. (A) Chromatograms, monitored at absorption of 210 nm (upper panel) and total ion intensity (lower panel), measured by optimized LC/TOFMS. The MS spectra of U3 (B), U4 (C), and U5 (D) and their possible chemical structures according to the accurate $m/z$ values of the predominant ions with TFA as an internal standard.

(DHAL) and 4-hydroxyallantoin (4-HAL) by using time-of-flight mass spectrometry (TOFMS). Two oxygen atoms were confirmed to be incorporated into the DIAA molecule by using $^{18}O_2$ and $H_2{}^{18}O$; one from $^1O_2$ and the other from water. Moreover, we isolated DIAA and 4-HAL and found that they gave PA and OUA as final products. We then presented a plausible reaction scheme.

## RESULTS AND DISCUSSION

**Photooxidation of UA.** In the presence of rose bengal (10 $\mu$M), an aqueous solution of UA (200 $\mu$M) was photoirradiated by UVA (1.12 mW/cm$^2$) for 2 h. UA and its oxidation products were measured by LC/TOFMS every 30 min during photooxidation. Figure 2A shows chromatograms of the reaction mixture after 60 min irradiation, monitored by the absorbance at 210 nm, and total ion intensity. In addition to UA, AL (impurity), PA (U1), OUA (U2), and unidentified products (U3, U4, and U5) were observed; the retention times of the unknowns were 5.4, 7.6, and 13.7 min, respectively. These compounds were also formed by 3-(1,4-dihydro-1,4-epidioxy-4-methyl-1-naphthyl)propionic acid (NEPO), which is a pure chemical $^1O_2$ generator, -initiated UA oxidation (data not shown) indicating that U3, U4, and U5 were $^1O_2$-induced UA oxidation products.

MS spectra of U3, U4, and U5 are shown in Figure 2B−D, and their accurate $m/z$ values were determined to be −199.01121, −155.01855, and −173.03023, respectively, using TFA as an internal standard. The molecular formulas of U3, U4, and U5 were determined as $C_5H_4N_4O_5$, $C_4H_4N_4O_3$, and $C_4H_6N_4O_4$, indicating that they were a peroxide derivative of UA, DHAL, and 4-HAL. Similar structures of DHAL and 4-HAL were proposed in the $^1O_2$-mediated oxidation of 8-oxoguanine.[8]

**Photooxidation of UA in $^{18}O_2$ and $H_2{}^{18}O$.** In order to characterize U3 more fully, we conducted the photooxidation in $^{18}O_2$. Figure 3B shows that the $m/z$ value for U3 shifted to −201.01459, indicating one atom of $^{18}O$ was incorporated. It is noteworthy that the peak at $m/z$ −199.01 was absent, suggesting that all air was replaced by $^{18}O_2$ and little $^{16}O_2$ was left. Similarly, PA, DHAL, and 4-HAL were monoisotopic (Figure 3A,C,D, insets show plausible locations for $^{18}O$ insertion).

Next, we conducted the photooxidation in $H_2{}^{18}O$ (Figure 4). PA, U3, DHAL, and 4-HAL were formed during UA oxidation similar to other oxidations. However, PA, U3, and 4-HAL were monoisotopic (Figure 4A,B,D, insets show plausible locations for $^{18}O$ insertion), whereas DHAL was not monoisotopic (Figure 4C). These results indicate that an O


DOI: 10.1021/acs.joc.9b00163
J. Org. Chem. 2019, 84, 3552−3558

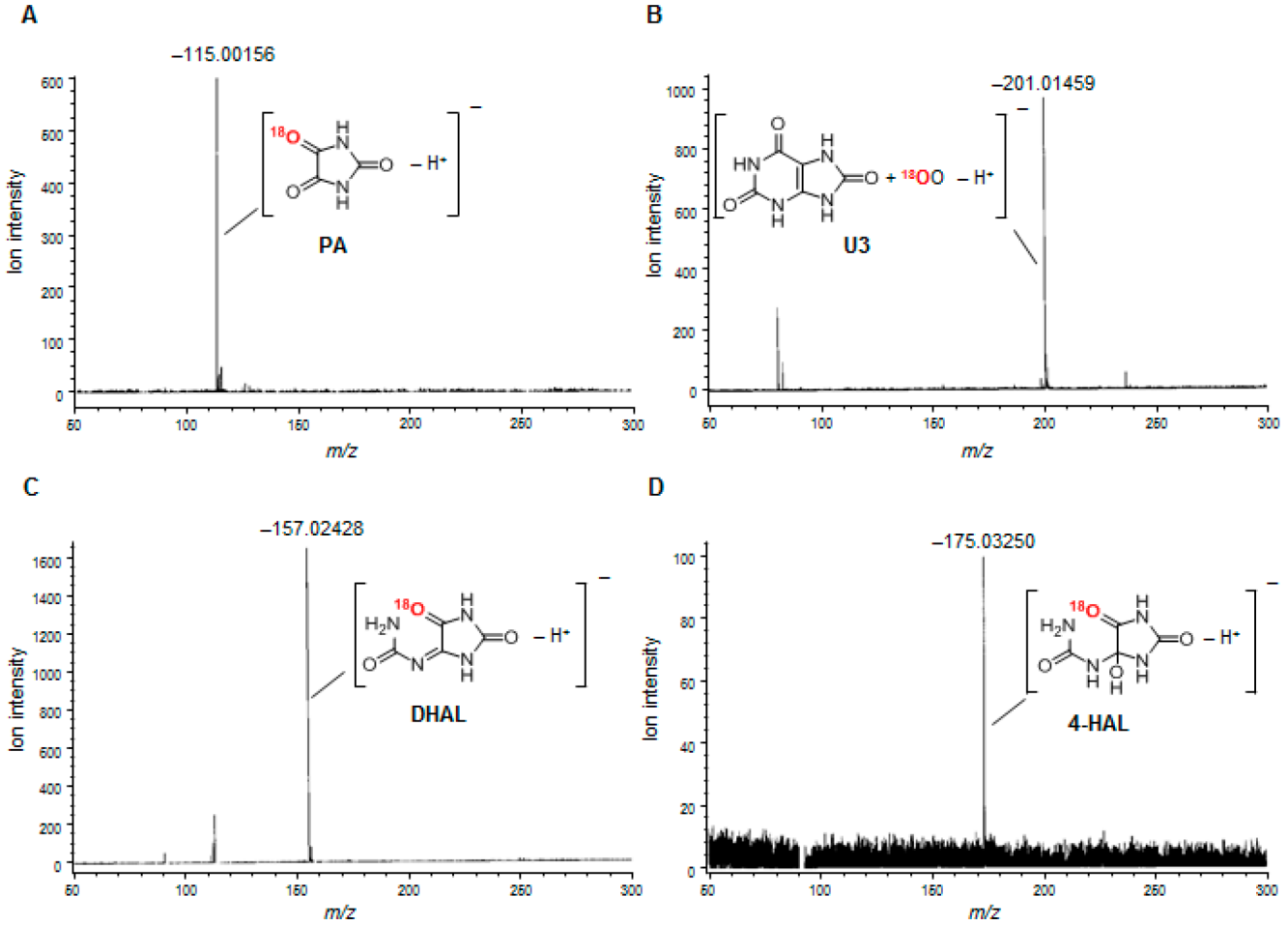


**Figure 3.** MS spectra of PA (A), U3 (B), DHAL (C), and 4-HAL (D) formed by UA photooxidation conducted under $^{18}O_2$ in $H_2O$. Measurements were carried out by LC/TOFMS, and the $m/z$ values were standardized against TFA.

atom incorporated to DHAL is derived from not water but $^1O_2$.

Taken together, these data confirm that U3 incorporated two oxygen atoms from the outside: one from $^1O_2$ and the other from water. From these results, a plausible reaction scheme based on a proposal by Duarte et al.[8] was proposed (Scheme 1). $^1O_2$ adds to UA, yielding UA-4,5-dioxetane (**1**). The 4,5-dioxetane is converted to UA-5-hydroperoxide (**2**). The nucleophilic addition of water on the C6 carbonyl carbon of UA-5-OOH results in cleavage of the peroxide and the C5−C6 bond to yield U3. U3 was determined to be DIAA. This scheme suggests that an oxygen atom from $^1O_2$ is incorporated in the 5-oxo- group and another oxygen atom from water is located on the carboxylic group of DIAA. DIAA is then converted either to DHAL by decarboxylation or to (4-hydroxy-2,5- dioxoimidazolidin-4-yl)aminocarbonylcarbamic acid (4-hydroxyDIAA) (**3**) by hydration. DHAL is hydrolyzed to 4-HAL, which decomposes to PA and urea. HDAA is rapidly converted to PA and *N*-carboxyurea.

**Analysis of DIAA Fragmentation.** To confirm the above scheme, fragmentation patterns of DIAA formed in $^{18}O_2$ and in $H_2{}^{18}O$ were compared. If the 5-oxo- and carboxylic oxygen atoms of DIAA are derived from $^1O_2$ and water, respectively (Figure 5A), their fragmentations can be distinguished. Collision-induced dissociation (CID) of DIAA ($m/z$ −199.00952) formed in normal air and water gave two typical fragment ions that were caused by decarboxylation ($m/z$ −155.02090) and further desorption of isocyanic acid ($m/z$ −112.01578) (Figure 5B). Figure 5C shows the fragmentation of the monoisotopic DIAA ($m/z$ −201.01460) formed in $^{18}O_2$. A monoisotopic fragment of decarboxylation ($m/z$ −157.02368) and a nonisotopic isocyanate desorption ion ($m/z$ −112.01543) were observed, indicating $^{18}O$ was incorporated in the dissociated isocyanate fragment. On the other hand, both fragment ions of the monoisotopic DIAA ($m/z$ −201.01576) produced in $H_2{}^{18}O$ were nonisotopic (Figure 5D), suggesting that $^{18}O$ located on the carboxylic group was primarily desorbed. These fragmentations were consistent with the proposed chemical structure and formation scheme of DIAA. Furthermore, UA photooxidation in DMSO led to a UA decrease without PA and DIAA formation (data not shown). It was suggested that PA and DIAA production requires water as an oxygen donor, and these observations also support the proposed scheme.

**Isolation and Incubation of DIAA and 4-HAL.** For further confirmation of the proposed scheme, DIAA and 4-HAL were isolated using HPLC since they were relatively stable. Incubation of these isolated compounds at neutral pH gave PA and OUA stoichiometrically as shown in Figure 6B,D. On the other hand, isolated DHAL was immediately converted into 4-HAL (data not shown).

The formation of urea was also observed during 4-HAL incubation, indicating that 4-HAL was the precursor of urea and PA. When DIAA was decomposed under weak acidic



DOI: 10.1021/acs.joc.9b00163
J. Org. Chem. 2019, 84, 3552−3558

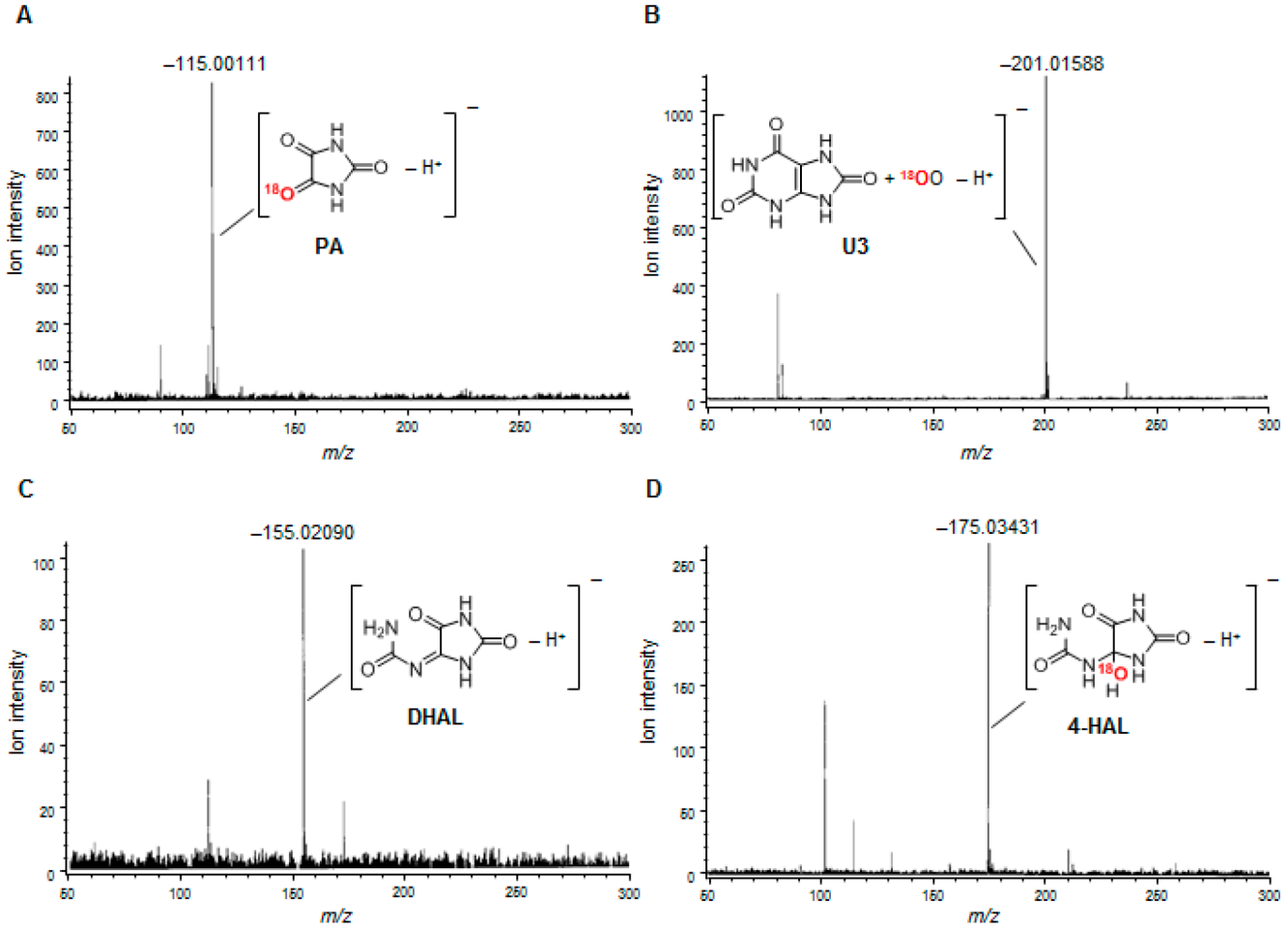


**Figure 4.** MS spectra of PA (A), U3 (B), DHAL (C), and 4-HAL (D) formed by UA photooxidation conducted under air in $H_2{}^{18}O$. Measurements were carried out by LC/TOFMS, and the *m*/*z* values were standardized against TFA.

**Scheme 1. Plausible Mechanism of PA Production by $^1O_2$-Induced UA Oxidation**

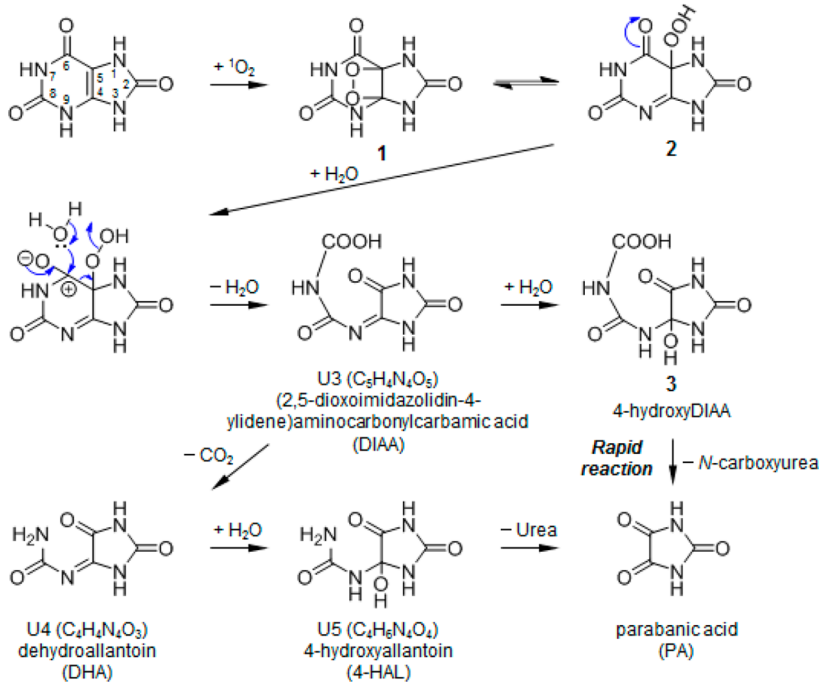




DOI: 10.1021/acs.joc.9b00163
J. Org. Chem. 2019, 84, 3552−3558

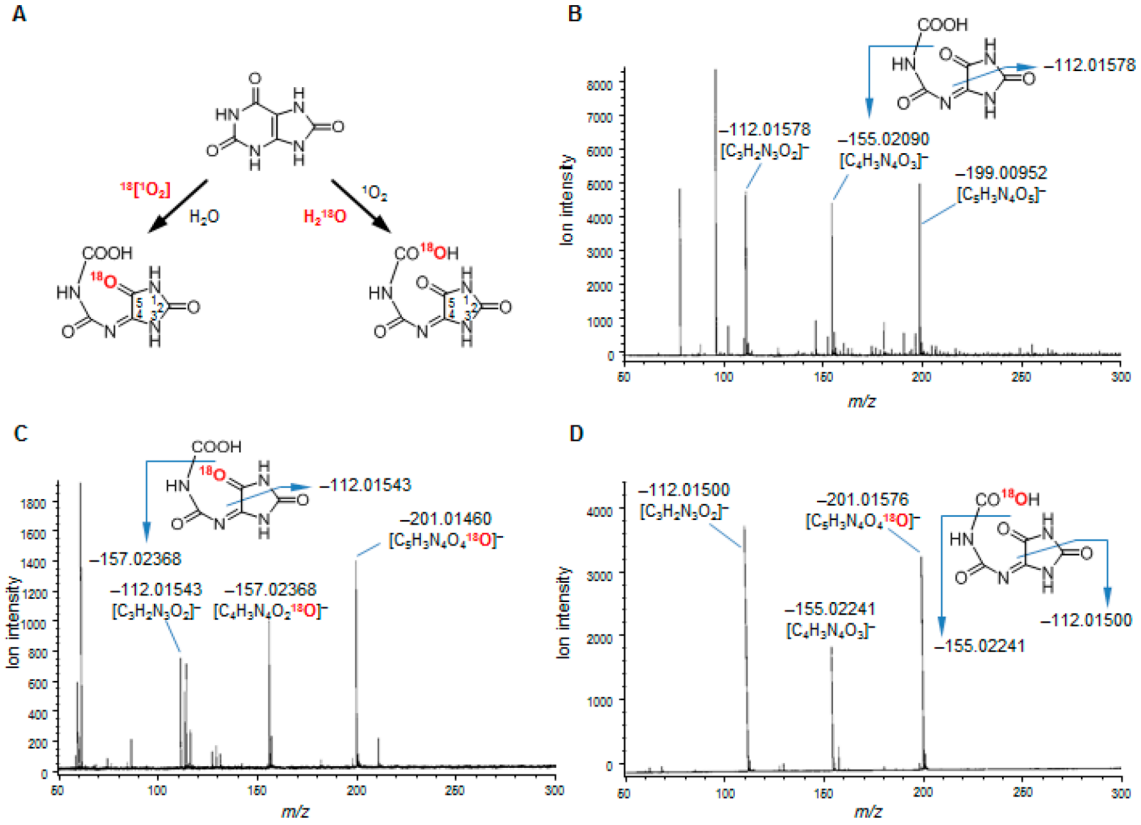


**Figure 5.** Fragmentation patterns of the DIAA measured by optimized LC/TOFMS. (A) Speculated $^{18}O$ atom location in DIAA molecule derived from $^{18}[^1O_2]$ (left arrow) or $H_2{}^{18}O$ (right arrow). The observed fragmentation of DIAA formed by UA photooxidation under normal air and in $H_2O$ (B), under $^{18}O_2$ and $H_2O$ (C), and under normal air and in $H_2{}^{18}O$ (D). The negative ionization was carried out by ESI with −2000 V of ionization potential. The *m/z* values were standardized against TFA as an internal standard, and postulated formulas showed their calculated *m/z* values to be within 5 millimass units from the observed values.

conditions (pH 5−6), DHAL production was observed in addition to PA formation (data not shown). It was shown that DIAA is the precursor of not only PA but also DHAL.

**Biological Significance.** Recently $^1O_2$-induced oxidation in vivo has attracted much interest. Umeno et al. reported that 10- and 12-(*Z,E*)-hydroxyoctadecadienoic acids (HODE), which are $^1O_2$-induced oxidation products of linoleic acid (LA), were detected in human plasma by LC/MS/MS analysis and the ratio of 10- and 12-(*Z,E*)-HODE to LA correlated significantly with several important clinical values for the diagnosis of diabetes, such as HbA1c, glucose, and insulin-related indices.[9] Furthermore, Hillered et al. showed that PA levels were elevated in serious aneurysmal subarachnoid hemorrhage.[10] These data suggest that $^1O_2$ may be produced in vivo under chronic diabetic conditions or acute severe brain damage. We expect that PA will be a good indicator for monitoring $^1O_2$ production in vivo and its importance will increase in the clinical fields.

## CONCLUSION

In the current study, the mechanism of PA formation with $^1O_2$-induced UA oxidation was fully characterized. We identified the chemical structure and formation pathway of DIAA, which is the key intermediate for PA production. Moreover, there are two pathways that branch out from DIAA leading to PA production: $H_2O$ addition and subsequently *N*-carboxyurea elimination directly yield PA and decarboxylation to give DHAL. DHAL is converted into 4-HAL, which is another precursor for PA formation. This characteristic mechanism is plausible for PA formation induced by $^1O_2$-initiated UA oxidation.

## EXPERIMENTAL SECTION

**Chemicals.** UA, PA, rose bengal, $H_2{}^{18}O$, and NEPO were purchased from Wako Pure Chemical Industries, Ltd. (Osaka, Japan), Tokyo Chemical Industry Co., Ltd. (Tokyo, Japan), or Waken B Tech Co., Ltd. (Kyoto, Japan) and used as received. OUA was prepared by hydrolysis of PA as described previously.[7] A super dehydrated grade ($H_2O$ content <0.001%) of dimethyl sulfoxide (DMSO) was used. The purity of the NEPO, which is a chemical $^1O_2$ generator, was determined as 78% by the comparison of the UV absorption at 288 nm before and after the thermal decomposition of a methanolic solution of NEPO. Pure $N_2$ and pure $^{18}O_2$ gases were purchased from Tomoe Shokai Co., Ltd. (Tokyo, Japan).

**UA Photooxidation.** In order to identify the oxidation products, the photooxidation of UA was carried out under various conditions. An aqueous solution containing 200 $\mu$M UA and 10 $\mu$M rose bengal was prepared and irradiated by UVA (1.12 mW/cm$^2$) for 2 h. During photooxidation, the mixture was analyzed every 30 min by a LC/TOFMS equipped with a UV detector. When the photooxidation under $^{18}O_2$ atmosphere was conducted, deoxygenation with $N_2$ bubbling was performed prior to the oxidation. The aqueous reaction mixture was poured into an airtight vial connected to a $N_2$ gas cylinder and a vacuum pump. $N_2$ gas was delivered into the well-stirred solution with vigorous bubbling for 3 h. Next, $^{18}O_2$ gas was induced into the vial using a vacuum pump. In the photooxidation in $H_2{}^{18}O$, the experimental solution was prepared with $H_2{}^{18}O$ as a solvent instead of water.



DOI: 10.1021/acs.joc.9b00163
J. Org. Chem. 2019, 84, 3552−3558

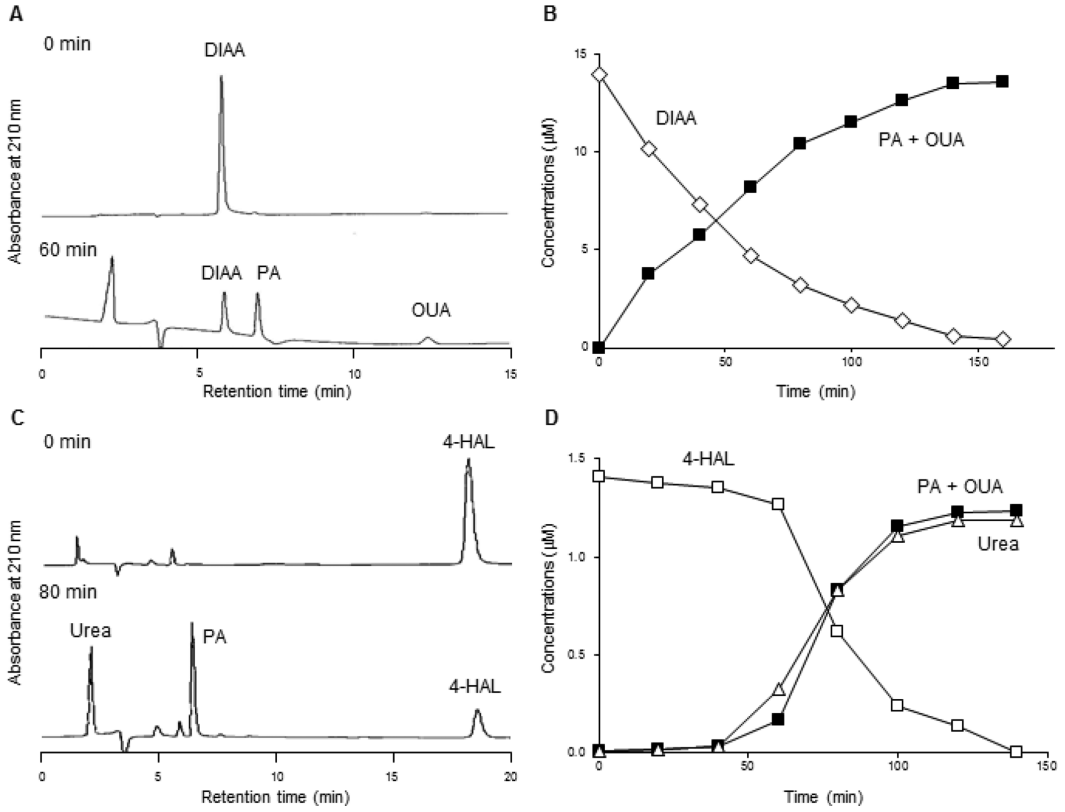


**Figure 6.** PA formation from the isolated DIAA and 4-HAL. (A) The chromatograms of DIAA immediately after isolation (upper panel) and after 60 min under neutral conditions (lower panel). (B) Time course of changes in the concentrations of PA plus OUA (■) and DIAA (◊) during storage at room temperature under neutral conditions. (C) Chromatograms of 4-HAL immediately after isolation (upper panel) and after 80 min under neutral conditions (lower panel). (D) Time course of changes in the concentrations of PA plus OUA (■), urea (△), and 4-HAL (□) during storage at room temperature under neutral conditions.

**NEPO-Initiated UA Oxidation.** UA was also oxidized by $^1O_2$ generated from thermal decomposition of NEPO as described previously.[7] Briefly, a methanolic solution of NEPO was added to UA aqueous solution. The reaction mixture containing 200 μM UA and 8 mM NEPO was incubated at 35 °C and analyzed by LC/TOFMS.

**HPLC Analysis.** A reversed-phase HPLC equipped with a UV detector was used for measuring and isolating UA oxidation metabolites. Water adjusted to pH 3.5 by formic acid was delivered at a rate of 1.0 mL/min as an isocratic mobile phase. A Develosil C30-UG (Nomura Chemical Co., Ltd., Tokyo, Japan), 5 μm, 250 mm × 4.6 mm, was used as a separation column.

**LC/TOFMS Analysis.** In order to obtain accurate mass-to-charge ratios ($m/z$) of UA oxidation products, an HPLC system (Agilent 1100 series, Agilent, Santa Clara, CA) equipped with a TOFMS (JMS-T100LC, JEOL Ltd., Tokyo, Japan) was used. Negative electrospray ionization (ESI) was performed at an ionization potential of −2000 V. The optimized applied voltages to ring lens, outer orifice, inner orifice, and ion guide were −5, −10, −5, and −500, respectively.

For measurements of fragmentation, those potentials were adjusted to −10, −50, −10, and −500 V. Trifluoroacetic acid (TFA) was used as an internal standard for $m/z$ calibration. HPLC separation was performed in the isocratic elution mode using a Develosil C30-UG (Nomura Chemical Co., Ltd., Tokyo, Japan), 5 μm, 250 mm × 2.0 mm, as a separation column and an aqueous mobile phase adjusted to pH 3.5 by formic acid delivered at 0.2 mL/min.

## AUTHOR INFORMATION


### Corresponding Author

*E-mail: afujisawa@stf.teu.ac.jp.

### ORCID

Akio Fujisawa: 0000-0001-7223-324X


### Notes

The authors declare no competing financial interest.

## REFERENCES


(1) Ames, B. N.; Cathcart, R.; Schwiers, E.; Hochstein, P. Uric acid provides an antioxidant defense in humans against oxidant- and radical-caused aging and cancer: a hypothesis. *Proc. Natl. Acad. Sci. U. S. A.* **1981**, *78* (11), 6858−6862.

(2) Hicks, M.; Wong, L. S.; Day, R. O. Identification of products from oxidation of uric acid induced by hydroxyl radicals. *Free Radical Res. Commun.* **1993**, *18* (6), 337−351.

(3) Robinson, K. M.; Morré, J. T.; Beckman, J. S. Triuret: a novel product of peroxynitrite-mediated oxidation of urate. *Arch. Biochem. Biophys.* **2004**, *423* (1), 213−217.

(4) Gersch, C.; Palii, S. P.; Imaram, W.; Kim, K. M.; Karumanchi, S. A.; Angerhofer, A.; Johnson, R. J.; Henderson, G. N. Reactions of peroxynitrite with uric acid: formation of reactive intermediates, alkylated products and triuret, and in vivo production of triuret under conditions of oxidative stress. *Nucleosides, Nucleotides Nucleic Acids* **2009**, *28* (2), 118−149.

(5) Gersch, C.; Palii, S. P.; Kim, K. M.; Angerhofer, A.; Johnson, R. J.; Henderson, G. N. Inactivation of nitric oxide by uric acid. *Nucleosides, Nucleotides Nucleic Acids* **2008**, *27* (8), 967−978.

(6) Iida, S.; Yamamoto, Y.; Susa, C.; Tsukui, K.; Fujisawa, A. 5-*N*-Carboxyimino-6-*N*-chloroaminopyrimidine-2,4(3*H*)-dione as a hypochlorite-specific oxidation product of uric acid. *J. Clin. Biochem. Nutr.* **2018**, *63* (2), 85−89.




DOI: 10.1021/acs.joc.9b00163
*J. Org. Chem.* 2019, 84, 3552−3558

(7) Iida, S.; Ohkubo, Y.; Yamamoto, Y.; Fujisawa, A. Parabanic acid is the singlet oxygen specific oxidation product of uric acid. *J. Clin. Biochem. Nutr.* **2017**, *61* (3), 169−175.
(8) Duarte, V.; Gasparutto, D.; Yamaguchi, L. F.; Ravanat, J. L.; Martinez, G. R.; Medeiros, M. H. G.; Di Mascio, P.; Cadet, J. Oxaluric acid as the major product of singlet oxygen-mediated oxidation of 8-oxo-7,8-dihydroguanine in DNA. *J. Am. Chem. Soc.* **2000**, *122* (51), 12622−12628.
(9) Umeno, A.; Shichiri, M.; Ishida, N.; Hashimoto, Y.; Abe, K.; Kataoka, M.; Yoshino, K.; Hagihara, Y.; Aki, N.; Funaki, M.; Asada, Y.; Yoshida, Y. Singlet oxygen induced products of linoleates, 10- and 12-(*Z*,*E*)-hydroxyoctadecadienoic acids (HODE), can be potential biomarkers for early detection of type 2 diabetes. *PLoS One* **2013**, *8* (5), e63542.
(10) Hillered, L.; Persson, L. Parabanic acid for monitoring of oxygen radical activity in the injured human brain. *NeuroReport* **1995**, *6* (13), 1816−1820.



DOI: 10.1021/acs.joc.9b00163
*J. Org. Chem.* 2019, 84, 3552−3558